Nonradiative Relaxation in Thiophene-S,S-dioxide Derivatives: The Role of the Environment

M. Anni,* F. Della Sala, M. F. Raganato, E. Fabiano, S. Lattante,† R. Cingolani, and G. Gigli

National Nanotechnology Laboratory (NNL) of INFM, Dipartimento di Ingegneria dell'Innovazione, Università degli Studi di Lecce, Via per Arnesano, 73100 Lecce, Italy

G. Barbarella and L. Favaretto

ISOF, Area della ricerca CNR, Via Gobetti 101, I-40129 Bologna, Italy

A. Görling

Institut für Physikalische und Theoretische Chemie, Wegelerstr. 12, D-55317 Bonn, Germany

Received: August 6, 2004; In Final Form: January 28, 2005

The intramolecular radiative and nonradiative relaxation processes of three thiophene-S,S-dioxide derivatives with different molecular rigidity are investigated in different solutions and in inert matrix. We show that the fluorescence quantum efficiency and the relaxation dynamics are strongly dependent on the environment viscosity, whereas they are almost independent of the environment polarity. We demonstrate that this strong dependence is due to an environment dependent nonradiative decay rate, whereas no relevant variations of the radiative decay rate are observed. We demonstrate that the dipole coupling with the solvent does not provide an efficient nonradiative decay channel and that the $S_n - S_1$ vibrational relaxation is very efficient in all of the molecules and for all of the investigated environments. Moreover first-principles time-dependent density-functional theory calculations in the correct, i.e., excited-state, molecular conformation, suggest that significant contributions of intersystem crossing to the triplet manifold can be excluded. We then conclude that the main nonradiative process determining the fluorescence quantum efficiency of this class of molecules is $S_1 - S_0$ internal conversion (IC). An explanation for the IC rate dependence in terms of the environment viscosity, molecular rigidity, $S_1 - S_0$ energy-gap, and molecular volume is presented.

I. Introduction

Thiophene based conjugated molecules receive great attention as active materials for low cost organic electronic devices, in particular field effect transistors (FET),[1−5] light emitting diodes (LED),[6−10] and solar cells.[11] Among the wide family of conjugated compounds, thiophene oligomers are characterized by high chemical stability[12] and wide tunability of the emission wavelength.[13] However, several properties of oligothiophenes, such as very low emission quantum efficiency in the solid phase, poor film forming properties, and low electron affinity, limit their applications to high-performance light emitting devices.

It has been recently demonstrated that a double oxidation of the central sulfur atom of the molecules allows one to overcome the limits of standard oligothiophenes. Recent results for the thienyl-S,S-dioxide oligothiophenes (TSOs), have revealed their wide color tunability,[14] fluorescence quantum efficiency in the solid state up to 70%,[15] high chemical stability,[16] increased electron affinity,[17] good solubility in common organic solvents, tunable optical gain,[18] and highly efficient lasing,[19,20] thus making the modified thiophenes appealing candidates for organic lasers and LEDs.

Quite surprisingly TSOs show lower emission efficiency for isolated molecules in solution than in the solid phase,[21,22] where instead intermolecular decay channels are usually expected to decrease the emission efficiency.[23,24] However, the origin of the strongly different emission properties of TSOs in the two different phases/environments is not completely understood, as the molecular functionalization affects both the intramolecular properties[25,26] and the intermolecular interactions.[21,27,28] The effects of the solvent and, more generally, of the external environment on the molecular relaxation processes in TSOs are thus still unclear.

The emission properties of organic molecules can be indeed strongly modified by the solvent polarity and viscosity.[29−36] Concerning thiophene based oligomers, it has been demonstrated that the emission properties, and in particular the fluorescence quantum efficiency, of standard oligothiophenes from two to seven rings are almost independent of the environment.[37] Similar results have been reported in naphthalene substituted oligothiophenes.[38] These studies also allowed to demonstrate that in oligothiophenes the main nonradiative process, which limits the emission efficiency, is intersystem crossing (ISC) to the triplets manifold, whereas $S_1 - S_0$ internal conversion (IC) plays a negligible role, as confirmed also by the study of oligothiophenes crystals[39] and by theoretical results.[40] On the contrary, it has been recently demonstrated that $S_1 - S_0$ IC plays a major role in the nonradiative relaxation in thiophene based polymers.[41,42] In thiophene-S,S-dioxide derivatives, the effects of the solvent polarity and viscosity are expected to be strong due to the electrostatic coupling between the SO_2 molecular dipole

* To whom correspondence should be addressed. E-mail: marco.anni@unile.it.

† Also at Dipartimento di Fisica, Università degli Studi di Lecce, Via per Arnesano, 73100 Lecce, Italy.

10.1021/jp046465j CCC: $30.25
Published on Web 03/04/2005

CHART 1: Chemical Structure of the Investigated Molecules

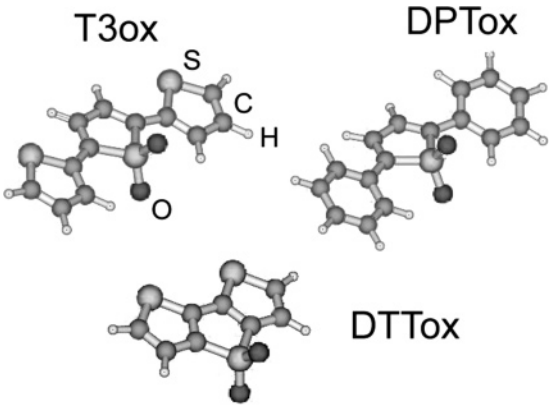

moment and the solvent[22] and the low torsional barrier that facilitates various conformational changes at room temperature of such oligomers.[43,44] Indeed, so far, only the behavior of a conformationally mobile quinquethiophene-S,S-dioxide has been analyzed by pump probe spectroscopy in a few solvents.[22] However, a deeper investigation on a wider class of systems and environments is required for a full understanding of the physical origin of the nonradiative processes.

In this work we investigate in detail the role of the environment on the photophysics of three dioxide trimers characterized by a different degree of molecular flexibility. The molecular structure of the three compounds, namely a dioxide terthiophene (T3ox), a dioxide diphenyl-thiophene (DPTox), and a rigid-core dioxide dithieno-thiophene (DTTox) are shown in Chart 1. The emission properties of the molecules are studied in dilute solutions as a function of the solvent polarity and viscosity, and in a poly(bisphenol A-carbonate) matrix.

We show that the fluorescence quantum efficiency and the relaxation dynamics are strongly affected by the environment viscosity for T3ox and DPTox but not for the rigid-core DTTox, whereas they are almost independent of the environment polarity. In low viscosity environments, the fluorescence quantum efficiency of the analyzed TSOs is lower than that of the corresponding non-oxygenated molecules,[37,45] but it increases up to a factor of 25 by increasing the viscosity due to the decrease of the total nonradiative rate (k_{nrad}). We demonstrate that this strong efficiency dependence on the environment is due to a variation of the nonradiative decay rate, whereas the radiative rate is almost independent of the environment.

We show that for all of the investigated molecules and environments the efficiency of the vibrational relaxation from the optically excited hot S_n^* state to the emitting S_1 is almost one, thus demonstrating that the environment strongly influences only the $S_1 - S_0$ relaxation.

In addition we show that, despite the permanent dipole of all of the molecules, dipole coupling with the solvent does not provide an efficient nonradiative decay channel.

Moreover first-principles calculations, based on time-dependent density-functional theory (TD-DFT), allow us to exclude also significant contributions of transfer to the triplet manifold by ISC.

These results strongly suggest that the main nonradiative process in dioxide oligothiophenes is $S_1 - S_0$ IC whose rate can be reduced by acting on the environment viscosity, the molecule rigidity, and the $S_1 - S_0$ energy gap.

Our results then indicate that the optical properties, and their environment dependence, of thiophene-S,S-dioxide derivatives are strongly different from what was previously reported in nonoxygenated thiophene based compounds, characterized by emission properties independent of the environment,[37,38] ISC to triplets as limiting process for the fluorescence quantum efficiency,[39,40] and absence of relevant $S_1 - S_0$ IC.

TABLE 1: Physical Properties of the Solvents Used in This Experiment, Namely Tetrahydrofuran (THF), Toluene, and Decalin[a]

solvent	ϵ	μ (D)	polarity (SPP)[46]	viscosity (mPa s)
THF	7.6	1.7	0.838	0.47
toluene	2.4	0.3	0.655	0.58
decalin	2.2	≈0	0.574	2.7

[a] The solvent polarity is expressed in the solvent polarity polarizability (SPP) scale.

II. Experimental Details

The molecular structures of the three investigated molecules are shown in Chart 1. As will be quantitatively discussed in section V the rigidity of the DPTox is higher than the T3ox one due to the stronger interaction with the central ring of the phenyl ring with respect to the thienyl one. The molecular rigidity is expected to be maximum in DTTox, characterized by external rings fused to the central one. Solutions were prepared with spectroscopic grade solvents without further purification. The physical properties of the solvents are reported in Table 1. To avoid intermolecular interactions, the concentration was decreased down to about 10^{-4} M. Inhert matrixes were realized by spin coating a chloroform solution of a blend of the active molecules with poly(bisphenol A-carbonate) (PC) with a mass ratio of 1:9. Films of thickness of about 3 μm were deposited by three sequential depositions to obtain layers with optical density around 1 at the excitation wavelength.

Continuous wave fluorescence (F) measurements were performed by exciting the samples with a continuous wave He−Cd laser (325 nm) and detecting the signal with a fiber-coupled Ocean Optics 2000 spectrometer, with a spectral resolution of about 10 nm. The fluorescence quantum efficiency was evaluated for the films (with higher emission) and for DTTox solutions by fixing them in an integrating sphere,[47] whereas for all the other solutions, with much lower emission, by comparing the signal with that of DTTox used as a standard.

The fluorescence excitation (FE) measurements were performed by a Varian Cary Eclipse fluorimeter.

Time-resolved fluorescence measurements were performed by exciting the samples with the second harmonic (390 nm) of a Mode Locked Ti−sapphire (Spectra Physics Tsunami), delivering 2 ps pulses with a repetition rate of 82 MHz. The signal was dispersed in wavelength and time by a spectrometer coupled with a streak camera and detected by a CCD. The overall temporal resolution was about 10 ps. To avoid temperature effects,[48] all of the measurements were performed at room temperature.

III. Computational Details

Theoretical calculations have been performed by first-principles methods based on TD-DFT, by using the parallelized quantum chemistry package TURBOMOLE.[49] We have optimized the ground state (S_0) and first singlet excited state (S_1) geometry. The geometry optimization of the emitting S_1 state allows us to calculate both the excitation and emission energies of the molecules (usually different due to geometrical relaxation in the excited state) and, see later on for details, the emission

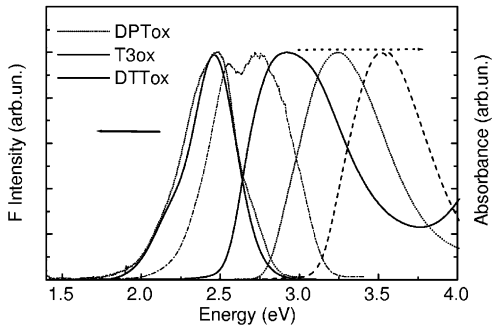

Figure 1. Fluorescence (F) and absorption spectra of the three molecules in THF. All the spectra are normalized to their peak value.

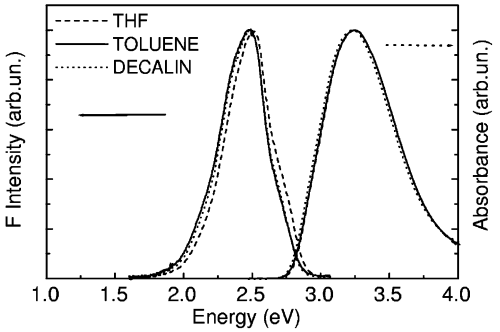

Figure 2. Fluorescence (F) and absorption spectra of DPTox solutions in solvents with different polarity. The spectra are normalized to their peak value.

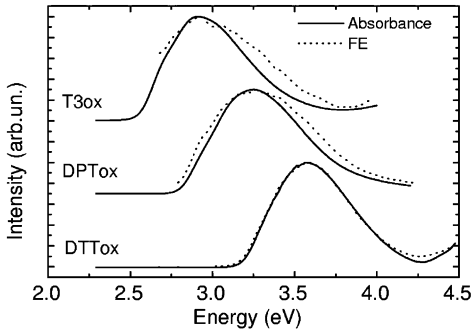

Figure 3. Comparison between the absorbance and excitation (FE) spectra for the three molecules in THF solutions.

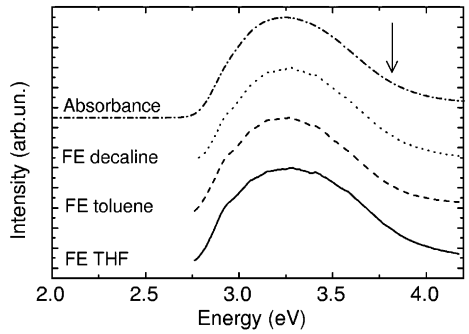

Figure 4. Dependence of the FE spectrum of DPTox on the solvent. No effects of the environment are visible. The arrow indicates the excitation energy in the efficiency measurements.

radiative lifetime. The S_1 excited state geometry has been obtained via the calculation of analytic TD-DFT gradients using the recently developed approach by Furche and Ahlrichs.[50] All geometries are found to be of C_{2v} symmetry except the ground-state of T3ox and DPTox, due to nonzero torsional angle of the external rings. Absorption energies and oscillator strengths have been obtained from TD-DFT calculations based on S_0 geometries, whereas the emission energies are the first singlet excitation energies in the S_1 geometries. We have used the hybrid B3LYP[51] exchange-correlation (XC) functional and the TZVP basis set[52] which is further augmented by one diffuse function for each angular momentum for first-row elements, both for geometry optimization and excitation energies.

For the investigation of the dependence of the S_0, S_1, T_1, and T_2 total energies on the torsional-angle, an SV(P)[53] basis set has been employed. The distorted geometries have been obtained from the optimized excited-state conformation by rotating the external rings and keeping the remaining coordinates frozen.

IV. Experimental Results

A. Fluorescence and Absorption Spectra. The fluorescence (F) and absorption spectra of the three molecules in THF solution are reported in Figure 1. The fluorescence and absorption spectra could be affected by the environment polarity, as all of the molecules present a permanent dipole due to the $S-O_2$ polar covalent bond. However, the spectral line shape and peak energy are almost independent of the environment polarity, as evidenced, for example, by the comparison of the DPTox spectra (normalized to their maximum intensity) in THF, toluene and decalin reported in Figure 2. The fluorescence spectra of the decalin and toluene solutions, with almost the same polarity, are only slightly red-shifted of about 5 nm (comparable with our spectral resolution), with respect to the THF solution, with very high polarity, but no evident solvatochromism is observed.

B. Fluorescence Excitation Spectra. When the molecules are excited to a highly excited hot singlet state S_n^* the excitation has to relax down to S_1 before radiative relaxation from S_1 to S_0 can occur. The fluorescence quantum efficiency, defined as the ratio between the number of emitted and absorbed photons, is then strongly dependent on the $S_n - S_1$ vibrational relaxation efficiency (usually almost one). To study the eventual presence of effects connected to the $S_n - S_1$ relaxation and to check their dependence on the environment, we compared absorbance and FE spectra (at the fluorescence peak wavelength) for all of the molecules (normalized to their peak value). The FE signal is infact dependent both on the density of excited states (as the absorbance) and on the efficiency of the relaxation from the excited state to the emitting one. The comparison of the obtained spectra in THF for the three molecules is reported in Figure 3. For all of the systems, the FE and absorbance spectra are almost identical, thus demonstrating that the Vavilov's rule[54] is satisfied and that the $S_n - S_1$ vibrational relaxation efficiency is almost one for the three molecules. This means that in all of the investigated molecules and in all of the investigated environments all of the excitation will decay by fast vibrational relaxation to the lowest emitting state S_1.

Moreover we analyzed the dependence of the FE and absorbance spectra on the solvent, reported in Figure 4 for DPTox. The spectra are independent of the environment and always almost identical, thus indicating that the $S_n - S_1$ vibrational relaxation efficiency is not affected by the environment.

C. Fluorescence Quantum Efficiency and Relaxation Dynamics. To have a deeper insight in the radiative and nonradiative decay processes of the investigated molecules, we analyzed the fluorescence efficiency and the relaxation dynamics in different environments. The fluorescence quantum efficiency of T3ox in THF is only 0.8% (see Figure 5), the efficiency of DPTox is slightly higher ($\eta_{PL} = 1.5\%$), whereas a very high

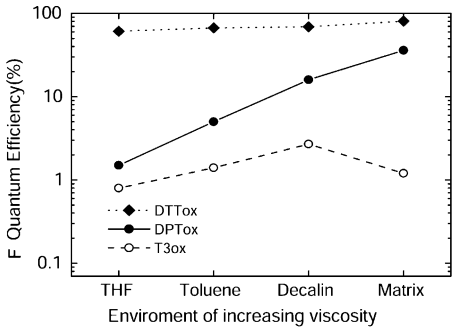

Figure 5. Absolute fluorescence quantum efficiency of the molecules in environments of increasing viscosity.

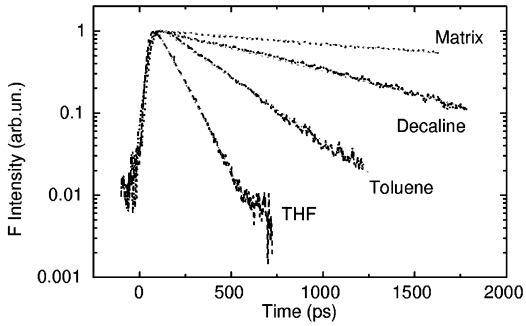

Figure 6. Time-resolved signal of DPTox in different environments. The dotted lines are the best fit curves with a monoexponential decay.

efficiency of 61% is observed for the rigid core molecule DTTox. It is important to observe that the efficiencies of T3ox and DPTox in solution are lower than that of the corresponding non-oxygenated molecules, which is 6% (ref 37) and 24% (ref 45), respectively. This result is inverted in the solid state, where the oxygen substitution allows one to strongly increase the emission efficiency with respect to standard oligothiophenes.[14,15]

In toluene solutions that are less polar and more viscous, the efficiency increases in T3ox and DPTox up to 1.4% and 5%, respectively, whereas the efficiency of DTTox is almost unchanged.

In Decalin solutions, which have almost the same polarity of toluene but a viscosity of about a factor of 5 higher, the efficiency strongly increases up to 2.7% for T3ox and up to 16% in DPTox, whereas the efficiency of the rigid molecule DTTox is again almost unchanged.

When the molecules are dispersed in the PC matrix, the emission efficiency is further increased up to 35% in DPTox and up to about 80% in DTTox, whereas a small reduction down to 1.2% is observed for T3ox.

These results clearly indicate that the relaxation processes of the nonrigid molecules are strongly affected by the environment properties. In particular, the strong efficiency increase of T3ox and DPTox from toluene to decalin solution suggests that the environment viscosity strongly influences the molecule relaxation. To analyze the effects of the environment on the radiative and nonradiative relaxation rates, we combined the quantum efficiency measurements with time-resolved fluorescence measurements.

The time-resolved fluorescence signal for DPTox is reported in Figure 6. The fluorescence decay is always monoexponential with a decay time (τ) increasing with the environment rigidity from 110 ps in THF to 2500 ps in PC matrix. The relaxation dynamics of T3ox is similar, with increasing lifetime as the solvent viscosity increases from about 80 ps in THF to about 390 ps in decalin solutions. On the contrary, the relaxation

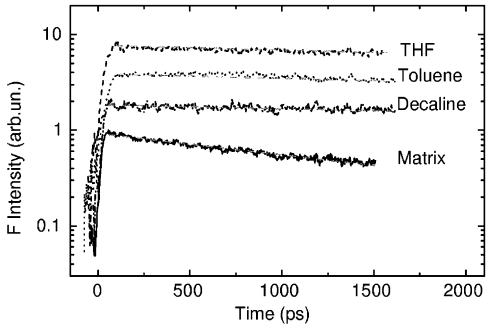

Figure 7. Time-resolved signal of DTTox in different environments. The dotted lines are the best fit curves with a monoexponential decay.

TABLE 2: Calculated Ground-state Properties for the Three Molecules: S_1 Excitation Energies, Oscillator Strengths (f), and Ground State Dipoles[a]

molecule	absorption (eV)	exp. absorption (eV)	f	dipole (D)
T3ox	2.70	2.93	0.59	2.76
DPTox	2.94	3.24	0.56	4.01
DTTox	3.53	3.53	0.18	4.60

[a] The experimental peak values of the absorption spectra are also reported.

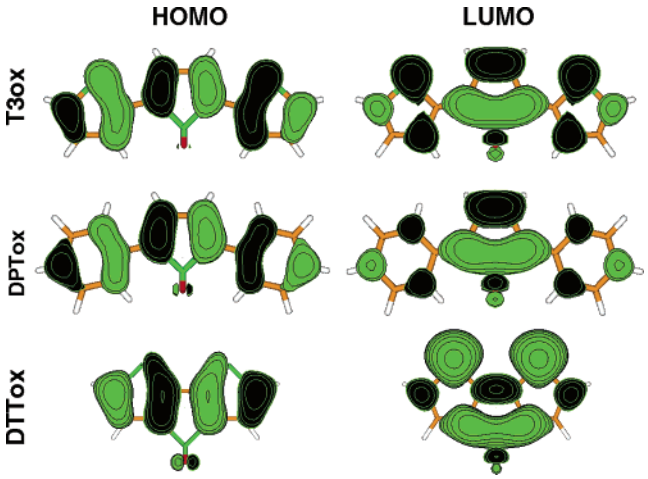

Figure 8. HOMO and LUMO wave functions for T3ox, DPTox, and DTTox (for the planar excited-state geometries).

dynamics of DTTox solutions, reported in Figure 7, shows a monoexponential decay with a decay time of about 10 ns almost independent of the solvent. A lifetime reduction down to 1.9 ns is instead observed in PC matrix.

V. Theoretical Results

The calculated S_1 excitation energies, oscillator strengths, and ground-state dipole moments are reported in Table 2. All of the S_1 transitions are almost completely characterized by electron promotion from the highest occupied molecular orbital (HOMO) to the lowest unoccupied molecular orbital (LUMO) and are polarized along the long molecular axis.

The HOMOs and LUMOs are displayed in Figure 8. The HOMOs and LUMOs of T3ox and DPTox are very similar to each other, both in the central and external rings. The orbitals for DTTox are similar to the central part of the ones for T3ox/DPTox. Thus, also from an electronic point of view, DTTox can be considered as a T3ox with fused rings. In DTTox, the electrons are more confined, and thus, the excitation energies are much higher than in T3ox/DPTox. Conversely, the length of DTTox and thus its oscillator strength is much reduced.

TABLE 3: Calculated Excited-State Properties for the Three Molecules: Emission Energies, Radiative Decay Times, Excited-State Dipoles, and Singlet−Triplet Splitting[a]

molecule	emission (eV)	exp. emission (eV)	τ_{rad} (ns)	dipole (D)	S_1-T_1 (eV)	S_1-T_2 (eV)
T3ox	2.08	2.46	11.0	3.02	1.67	−0.37
DPTox	2.21	2.49	10.2	4.09	1.58	−0.59
DTTox	2.73	2.73	21.6	5.32	1.39	−0.67

[a] The experimental peak energy of the fluorescence spectra is also reported.

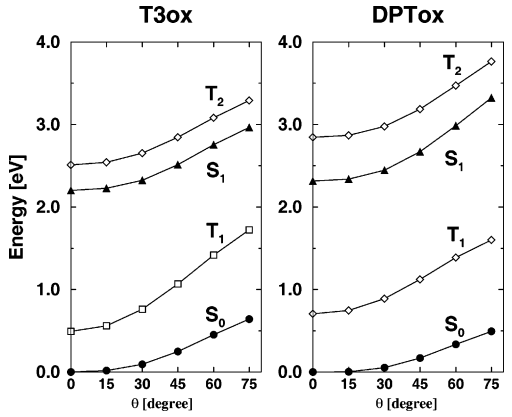

Figure 9. S_0, S_1, T_1, T_2 potential energy surface in eV versus inter-ring torsional angle for T3ox, DPTox with the B3LYP/SV(P) approach. The total energies are given relative to the S_0 total energy at zero inter-ring torsional angle.

The emission energy, the radiative lifetime, the excited-state dipole, and the energy difference between S_1, the closest triplet T_2, and the triplet T_1 are reported in Table 3. The radiative lifetime τ_{rad} has been obtained using the Einstein relation $\tau_{rad} = 23.01/(f E^2)$, where f is the excited-state oscillator strength, E is the emission energy in eV, and τ_{rad} is in nanoseconds. Note that this Einstein relation holds only for two-level systems. It can be applied to the presented molecules because these molecules are characterized by the S_1 state well separated in energy from other states and thus are well represented as two-level systems. For each system, the excited-state dipole is found to be very close to the ground-state dipole as the transition dipole is orthogonal to the ground-state dipole.

A qualitative description of the ISC rate can be performed as a function of the energy separation between the singlet S_1 and the closest triplet T_n,[25,39,40,55] as the ISC rate exponentially decreases as the singlet−triplet gap increases.[57] Differently than in previous approaches, in this paper, we use the $S_1 - T_n$ energy at the correct potential surface position, i.e., the S_1 minimum. From the values reported in Table 3, it is evident that the triplet state closest to S_1 is, for all of the molecules, T_2, whereas the $S_1 - T_1$ energy gap is very large (about 1.5 eV). For all of the molecules, the highest contribution to the total ISC rate is thus given by the $S_1 - T_2$ rate.

For all of the investigated molecules, the $S_1 - T_2$ energy gaps are negative, thus indicating that T_2 is at higher energy than S_1 and much higher than the thermal energy kT in all of the molecules. The excitation transfer to the triplet manifold by ISC is then a thermally activated process but with an activation energy much higher than kT at room temperature.

To investigate the eventual presence of torsional effects on the excited states energy, we determined the S_0, S_1, T_1, and T_2 total energies as function of the inter-ring torsional angle θ for T3ox and DPTox (Figure 9). The total energies are given relative to the S_0 total energy at no torsion angle. Thus, the values at $\theta = 0°$ represent emission energies. The latter are higher by about 0.1 eV than those listed in Table 3 due to the smaller basis set employed for the investigation of the torsional effects (see Section 3).

TABLE 4: Comparison between the Experimental and Theoretical Stokes Shift

molecule	experimental Stoke shift (eV)	theoretical Stoke shift (eV)
T3ox	0.46	0.62
DPTox	0.78	0.73
DTTox	0.80	0.83

Figure 9 shows that, although total energies are strongly affected by θ, their differences, i.e., the transition energies, are much less so. In particular the $S_1 - T_2$ energy gap, which mainly determines the ISC rate, is almost constant: it increases by only 0.02 eV for T3ox and 0.09 eV for DPTox from $\theta = 0°$ to 75°.

Finally we estimated the molecular rigidity in the excited state with respect the inter-ring torsion angle, which can be defined as

$$R = \frac{1}{2}\frac{\partial^2 E_{S_1}}{\partial \theta^2} \qquad (1)$$

Parabolic fits of the S_1 curves in Figure 9 give 1.399 10^{-4} eV/degree^2 and 1.832 10^{-4} eV/degrees^2 for T3ox and DPTox, respectively.

In DPTox the later ring is a phenyl which is larger than the thiophene ring of T3ox, and thus, it has a stronger interaction with the central ring. This explains the larger molecular rigidity of DPTox with respect T3ox.

The previous definition of the molecular rigidity cannot be applied to DTTox, due to the fusion of rings. A more precise and quantitative analysis is the evaluation of the lowest vibrational frequencies in the excited state, which will be investigated elsewhere.

VI. Discussion

A. Emission and Absorption Spectra. The experimental peak energies of both fluorescence and absorption are in excellent agreement with the theoretical values for DTTox, whereas deviations in the range 0.2−0.3 eV are observed for DPTox and T3ox. This generally good agreement between the theoretical and experimental value allows us to assign the experimental peaks to the S_1 molecular state. In Table 4, the experimental Stokes shifts are reported and compared to the theoretical values. The Stokes shifts are quite large and larger than the ones in nonoxygenated systems.[37,45] This effect is not related to extrinsic effects such as aggregate formation and solvent effects, but it is an intrinsic molecular property related to conformational changes in the excited-state as confirmed by the very good agreement between the calculated and experimental values.

The observed independence of the fluorescence and absorption spectra on the solvent polarity is due to the absence of a strong dipole difference between the ground and the first excited state,[56] described in section V.

B. Fluorescence Efficiency and Relaxation Dynamics. The comparison of the absorbance and excitation spectra demonstrates that the fluorescence efficiency in the three investigated molecules is not affected by $S_n - S_1$ nonradiative vibrational relaxation, as the efficiency of this process is one for all of the molecules and the environments. The observed environment dependence of the fluorescence efficiency has then to be ascribed

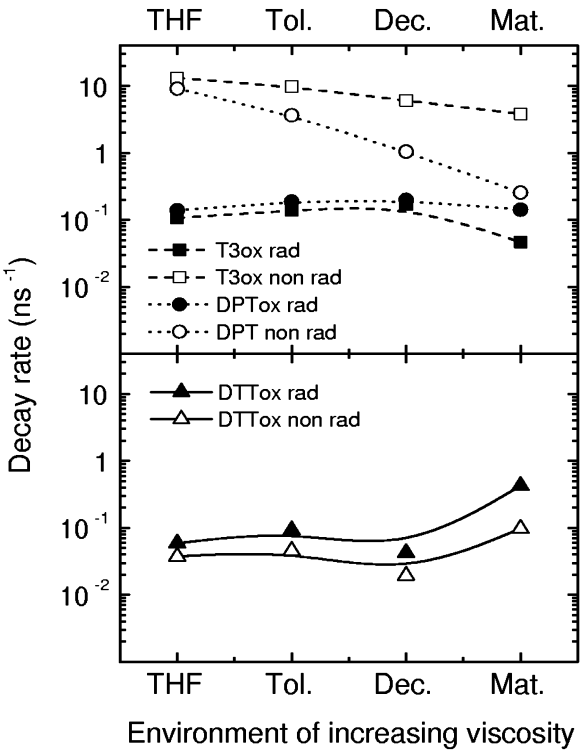

Figure 10. Radiative (empty symbols) and nonradiative (full symbols) decay rates of the three molecules in different environments. The data of DTTox are reported in a separate plot with the same scale for clarity.

to the dependence on the environment of the $S_1 - S_0$ relaxation. Such dependence can be due to an environment dependence of the radiative decay rate or of the nonradiative one, or both.

The simultaneous knowledge of the fluorescence decay rate $k = 1/\tau$ and the emission efficiency η_F allows us to determine the radiative (k_{rad}) and nonradiative (k_{nrad}) $S_1 - S_0$ decay rates through the relations

$$k = k_{rad} + k_{nrad} \quad (2)$$

$$\eta_F = \frac{k_{rad}}{k} \quad (3)$$

The radiative and nonradiative decay rates of all of the molecules in the different investigated environments are reported in Figure 10. The radiative rate is almost independent of the environment for all of the molecules, with the only exception of a decreased radiative rate in T3ox:PC matrix. This last result together with the decreased fluorescence efficiency and a red-shift of about 230 meV in the fluorescence spectrum with respect to the molecules in solution indicates that the T3ox matrix emission is partially due to interacting molecules (aggregates). It is also important to observe that, despite the different molecular structure, the radiative rates of the three molecules are, in any environment, of the same order of magnitude (about 10^{-1} ns^{-1}).

For all of the three molecules, the theoretical values of the radiative rate are in excellent agreement with the experimental values, as shown in Figure 11. This agreement is not trivial as τ_{rad} relates calculated emission energy and oscillator strength to measured fluorescence lifetimes and efficiencies and indicates that the studied emission properties in solution are the single molecule properties.

Differently from the radiative decay rate, the nonradiative rate is observed to decrease, both in DPTox and T3ox, as the environment rigidity increases, thus demonstrating that the

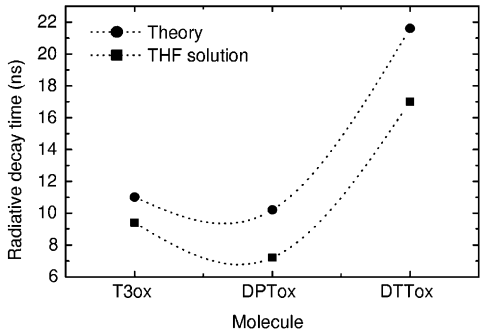

Figure 11. Comparison between the theoretical and experimental radiative decay time.

observed fluorescence efficiency increase is due to the progressive suppression of some nonradiative decay processes. The nonradiative decay rate of the rigid molecule DTTox is instead almost independent of the solvent, and slightly increased in PC matrix.

By comparing the k_{nrad} value of the three molecules in a fixed environment it is also evident that k_{nrad} decreases as the molecule rigidity increases, as for all of the environments $k_{nrad}^{DTTox} < k_{nrad}^{DPTox} < k_{nrad}^{T3ox}$.

These results demonstrate that the environment dependence of the fluorescence quantum efficiency is due to the environment dependence of the total nonradiative decay rate. Moreover, the absence of a k_{nrad} dependence on the solvent properties in the rigid core molecule DTTox, together with the strong k_{nrad} decrease of T3ox and DPTox with the solvent viscosity, indicates that the nonradiative decay rate decreases with the increase of the molecule and/or environment rigidity. These results are very different from what was observed in solution both in standard oligothiophene and in naphthalene substituted oligothiophenes, showing a fluorescence quantum efficiency independent of the solvent properties.[37,38]

C. Origin of the Nonradiative Ralaxation. The three relaxation processes which have to be included in the total nonradiative rate k_{nrad} are dipole−dipole coupling with the solvent, ISC to the triplet manifold, and $S_1 - S_0$ IC.

An efficient dipole−dipole coupling with the solvent cannot be a priori excluded due to the permanent dipole moment of our molecules, due to the same S−O_2 covalent bond. However, despite the similar dipole moment (see Table 2) of the three molecules, η_F of DTTox is always very high and much higher that η_F of T3ox and DPTox. Moreover no relevant dependence of the fluorescence and absorption spectra in the solvent polarity has been observed. This demonstrates that the nonradiative dipole−dipole coupling with the solvent molecules is not the main nonradiative process in our molecules, so it is not the process limiting the fluorescence quantum efficiency.

The observed dependence of the emission properties on both the molecular structure and the environment has then to be ascribed to $S_1 - S_0$ Internal Conversion (IC) and/or Intersystem Crossing to the triplets manifold. The total non radiative decay rate k_{nrad} has then to be expressed as $k_{nrad} = k_{ISC} + k_{IC}$.

To quantify the relative importance of IC and ISC on the nonradiative relaxation of thiophene-S,S-dioxide derivatives, a direct measurement of the ISC quantum yield is necessary. These kinds of measurements have been used to demonstrate that ISC is the main nonradiative decay process in standard oligothiophenes,[37] while important contribution of $S_1 - S_0$ IC have been observed in polythiophenes.[41,42]

Even if these measurements are not present in this paper, it is anyway possible to qualitatively discuss the relative impor-

tance of IC and ISC by combining the experimental and theoretical results. In particular, several elements strongly suggest that the ISC is not the main nonradiative decay process in our class of molecules, as previously directly demonstrated by Lanzani et al.[22] by pump and probe measurements on solutions of a dioxide quinquethiophene:

(1) The oxygen functionalization of the sulfur atom strongly reduces the ISC rate due to the increase of the $S_1 - T_2$ energy gap, as reported in Table 3, and due to the reduction of the central sulfur atom contribution in the LUMO.[25,26] In our molecules the calculated $S_1 - T_2$ energy gap is in the range 370÷670 meV, which is much larger than kT at room temperature, suggesting that important effects due to singlet exciton ISC to triplets should be excluded in all of the molecules.[25,40]

(2) Despite the prediction of reduced ISC rate, the fluorescence efficiencies of DPTox and T3ox in THF are lower than those of the corresponding nonoxygenated molecules. This strongly suggest that ISC is not the main non radiative process in our molecules.

(3) The total nonradiative rate k_{nrad} clearly decreases with the molecule and/or environment rigidity. Torsional effects on the ISC rate can be in general observed, if the $S_1 - T_n$ energy gap depends on the molecule geometry. However, our theoretical results indicate that, in both T3ox and DPTox, the $S_1 - T_2$ energy gap is almost independent of the molecule torsion. The ISC rate is then predicted to be independent of the molecular torsion and then the ISC rate to be independent of the environment viscosity.

Our experimental findings can be instead well explained by assuming that the main nonradiative process is $S_1 - S_0$ IC whose rate (k_{IC}), according to the phenomenological theory of Sharafy and Muszkat,[30] depends on the viscosity through the relation

$$k_{IC} = k_{IC}^0 \left(\frac{\eta_0}{\eta}\right)^a \tag{4}$$

where k_{IC}^0 decreases with the $S_1 - S_0$ gap[57,58] and with the molecule rigidity, whereas a depends on the volume of the displaced solvent. The k_{IC} dependence on the $S_1 - S_0$ energy gap and on the volume of displaced solvent allows us to fully explain the experimental dependence of k_{nrad} on the environment viscosity, in particular:

(1) For a given viscosity, the IC rate is higher in the TSOs molecules than in the unsubstituted ones due to the decrease of the $S_1 - S_0$ gap induced by the dioxide group. This explains the very low efficiency in low viscosity solution of T3ox and DPTox.

(2) The lower $S_1 - S_0$ gap of the oxygenated molecules T3ox and DPTox with respect to the corresponding nonoxygenated ones T3 and DPT[21,22] (and characterized by similar, low torsional barriers) determines also their strong fluorescence efficiency increase with the environment viscosity.

(3) On the contrary, DTTox shows very high fluorescence efficiency independent of the environment viscosity as the molecule rigidity is increased by the fusion of the external rings to the central one.

(4) The larger relative increase of the fluorescence efficiency in DPTox with respect to T3ox with the viscosity, which is surprising if only the molecular rigidity (which is very low in both molecules but larger for DPTox) is taken into account, is instead related to the volume of the displaced solvent. The larger volume of the phenyl rings with respect to the thienyl ones results in a larger volume of displaced solvent due to the vibrations in DPTox than T3ox, which determines a higher value of a.

VII. Conclusions

We studied the photophysics of thiophene-S,S-dioxide derivatives in different environments demonstrating that the relaxation processes in this class of molecules strongly depend on the environment.

We showed that the efficiency increases as the environment viscosity increases, due to the decrease of the nonradiative decay rate, whereas the radiative decay rate is found to be independent of the environment. Moreover we demonstrated that the radiative rates of the three molecules are always similar, whereas the nonradiative rate decreases as the molecule rigidity increases. In addition, we demonstrated that the environment does not influence the $S_n^* - S_1$ vibrational relaxation efficiency, which is almost one for all of the molecules in all of the investigated environments. We also showed that, despite the permanent dipole of all the molecules, dipole coupling with the solvent does not provide an efficient nonradiative decay channel.

These results demonstrate that the two most important nonradiative relaxation processes, affected by the environment and by the molecular structure, are $S_1 - S_0$ IC and ISC to the triplet manifold. Even if a direct measurement of the ISC quantum yield is necessary to exactly quantify the relative importance of these two processes, we showed that our results, both experimental and theoretical, strongly suggest that no significant contributions of transfer to the triplet manifold by ISC are present.

Our results can be instead well, qualitatively, explained assuming that the main nonradiative decay process in the molecules is $S_1 - S_0$ IC.

The $S_1 - S_0$ IC rate increases in the oxygenated molecules due to the decreased $S_1 - S_0$ energy gap induced by the oxygen functionalization. We also showed that the $S_1 - S_0$ IC rate can be reduced by acting on the environment viscosity, the molecule rigidity, and the $S_1 - S_0$ energy gap.

Acknowledgment. We thank R. Ahlrichs for providing the TURBOMOLE program package and G. Aloisio for his support. Simulations have been performed at the CACT-ISUFI (Lecce).

References and Notes

(1) Horowitz, G.; Fichou, D.; Peng, X.; Wu, Z.; Garnier, F. *Solid State Commun.* **1989**, *72*, 381.

(2) Garnier, F.; Horowitz, G.; Fichou, D.; Peng, X. *Adv. Mater.* **1990**, *2*, 592.

(3) Dodabalapur, A.; Katz, H. E.; Torsi, L.; Haddon, R. C. *Appl. Phys. Lett.* **1996**, *68*, 1108.

(4) Dodabalapur, A.; Katz, H. E.; Torsi, L.; Haddon, R. C. *Science* **1995**, *269*, 1560.

(5) Halik, M.; Klauk, H.; Zschieschang, U.; Schmid, G.; Ponomarenko, S.; Kyrchmeier, S.; Weber, W. *Adv. Mater.* **2003**, *15*, 917.

(6) Horowitz, G.; Delannoy, P.; Bouchriha, H.; Deloffre, F.; Fave, J. L.; Garnier, F.; Hajlaoui, R.; Heyman, M.; Kouki, F.; Valat, P.; Wintgens, V.; Yassar, A. *Adv. Mater.* **1994**, *6*, 752.

(7) Uchiyama, K.; Akimichi, H.; Hotta, S.; Noge, H.; Sakaki, H. *Synth. Met.* **1994**, *63*, 57.

(8) Noda, T.; Ogawa, H.; Noma, N.; Shirota, Y. *Appl. Phys. Lett.* **1997**, *70*, 699.

(9) Shirota, Y.; Kinoshita, M.; Noda, T.; Okumoto, K.; Ohara, T. *J. Am. Chem. Soc.* **2000**, *122*, 11021.

(10) Doi, H.; Kinoshita, M.; Okumoto, K.; Shirota, Y. *Chem. Mater.* **2003**, *15*, 1080.

(11) Ackermann, J.; Videlot, C.; El Kassmi, A. *Thin Solid Films* **2002**, *403−404*, 157.

(12) Ziegler, C. In *Handbook of Organic Conductive Molecules and Polymers*; Nalwa, H. S., Ed.; Wiley: New York, 1997; Vol. 3, Chapter 13.

(13) Berggren, M.; Inganas, O.; Gustaffson, G.; Rasmusson, J.; Andersson, M. R.; Hjertberg, T.; Wennerstrom, W. *Nature* **1994**, *372*, 444.
(14) Barbarella, G.; Favaretto, L.; Sotgiu, G.; Zambianchi, M.; Bongini, A.; Arbizzani, C.; Mastragostino, M.; Anni, M.; Gigli, G.; Cingolani, R. *J. Am. Chem. Soc.* **2000**, *122*, 11971.
(15) Anni, M.; Gigli, G.; Paladini, V.; Cingolani, R.; Barbarella, G.; Favaretto, L.; Sotgiu, G.; Zambianchi, M. *Appl. Phys. Lett.* **2000**, *77*, 2458.
(16) Barbarella, G.; Favaretto, L.; Zambianchi, M.; Pudova, O.; Arbizzani, C.; Bongini, A.; Mastragostino, M. *Adv. Mater.* **1998**, *10*, 551.
(17) Barbarella, G.; Favaretto, L.; Sotgiu, G.; Zambianchi, M.; Fattori, V.; Cocchi, M.; Cacialli, F.; Gigli, G.; Cingolani, R. *Adv. Mater.* **1999**, *11*, 1375.
(18) Anni, M.; Gigli, G.; Zavelani-Rossi, M.; Gadermaier, C.; Lanzani, G.; Barbarella, G.; Favaretto, L.; Cingolani, R. Electronic, Optical and Optoelectronic Polymers and Oligomers Symposium. *Mater. Res. Soc. Symp. Proc.* **2002**, *665*, 29.
(19) Pisignano, D.; Anni, M.; Gigli, G.; Zavelani-Rossi, M.; Lanzani, G.; Barbarella, G.; Favaretto, L.; Cingolani, R. *Appl. Phys. Lett.* **2002**, *81*, 3534.
(20) Zavelani-Rossi, M.; Lanzani, G.; De Silvestri, S.; Anni, M.; Gigli, G.; Cingolani, R.; Barbarella, G.; Favaretto, L. *Appl. Phys. Lett.* **2001**, *79*, 4082.
(21) Barbarella, G.;, Zambianchi, M.; Antolini, L.; Ostoja, P.; Maccagnani, P.; Bongini, A.; Marseglia, E. A.; Tedesco, E.; Gigli, G.; Cingolani, R. *J. Am. Chem. Soc.* **1999**, *121*, 8920.
(22) Lanzani, G.; Cerullo, G.; De Silvestri, S.; Barbarella, G.; Favaretto, L. *J. Chem. Phys.* **2001**, *115*, 1623.
(23) Yassar, A.; Horowitz, G.; Valat, P.; Wintgens, V.; Hmyene, M.; Deloffre, F.; Srivastava, P.; Lang, P.; Garnier, F. *J. Phys. Chem.* **1995**, *99*, 9155.
(24) Oelkrug, D.; Egelhaaf, H. J.; Gierschner, J.; Tompert, A. *Synth. Met.* **1996**, *76*, 249.
(25) Della Sala, F.; Heinze, H. H.; Görling, A. *Chem. Phys. Lett.* **2001**, *339*, 343.
(26) Raganato, M. F.; Vitale, V.; Della Sala, F.; Anni, M.; Cingolani, R.; Gigli, G.; Favaretto, L.; Barbarella, G.; Weimer, M.; Göorling, A. *J. Chem. Phys.* **2004**, *121*, 3784.
(27) Antolini, L.; Folli, U.; Goldoni, F.; Mucci, A.; Schenetti, L. *Acta Polym.* **1998**, *49*, 248.
(28) Tedesco, E.; Della Sala, F.; Favaretto, L.; Barbarella, G.; Albesa-Jové, D.; Pisignano, D.; Gigli, G.; Cingolani, R.; Harris, K. D. M. *J. Am. Chem. Soc.* **2003**, *125*, 12277.
(29) Kummer, A.; Kompa, C.; Niwa, H.; Hirano, T.; Kojima, S.; Michel-Beyerele, M. E. *J. Phys. Chem. B* **2002**, *106*, 7554.
(30) Sharafy, S.; Muszkat, K. A. *J. Am. Chem. Soc.* **1971**, *93*, 4119.
(31) Dey, J.; Warner, I. M. *J. Phys. Chem. A* **1997**, *101*, 4872.
(32) Jacobson, A.; Petric, A.; Hogenkamp, D.; Sinur, A.; Barrio, J. R. *J. Am. Chem. Soc.* **1996**, *118*, 5572.
(33) Sun, Y. P.; Ma, B. *Chem. Phys. Lett.* **1995**, *236*, 285.
(34) Burget, D.; Jacques, P. *Chem. Phys. Lett.* **1998**, *291*, 207.
(35) Jones, G., II; Jackson, W. R.; Choi, C. Y.; Bergmark, W. R. *J. Phys. Chem.* **1985**, *89*, 295.
(36) Pavlovish, V. S. *J. Lumin.* **2000**, *87*−*89*, 592.
(37) Becker, R. S.; Seixas de Melo, J.; Macanita, A. L.; Elisei, F. *J. Phys. Chem.* **1996**, *100*, 18683.
(38) Seixas de Melo, J.; Silva, L. M.; Kuroda, M. *J. Chem. Phys.* **2001**, *115*, 5625.
(39) Gigli, G.; Della Sala, F.; Lomascolo, M.; Anni, M.; Barbarella, G.; Di Carlo, A.; Lugli, P.; Cingolani, R. *Phys. Rev. Lett.* **2001**, *86*, 167.
(40) Belijonne, D.; Cornil, J.; Friend, R. H.; Janssen, R. A. J.; Brédas, J. L. *J. Am. Chem. Soc.* **1996**, *118*, 6453.
(41) Seixas de Melo, J.; Burrows, H. D.; Svensson, M.; Andersson, M. R.; Monkman, A. P. *J. Chem. Phys.* **2003**, *118*, 1550.
(42) Huang, Y.-F.; Chen, H.-L.; Ting, J. W.; Liao, C.-S.; Larsen, R. W.; Fann, W.; *J. Phys. Chem. B* **2004**, *108*, 9619.
(43) Smilowitz, L.; Hays, A.; Heeger, A. J.; Wang, W.; Bowers, J. E. *J. Chem. Phys.* **1993**, *98*, 6504.
(44) Oelkrug, D.; Tompert, A.; Gierschner, J.; Egelhaaf, H.-J.; Hanack, M.; Hohloch, M.; Steinhuber, E. *J. Phys. Chem. B* **1998**, *102*, 1902.
(45) Lee, S. A.; Hotta, S.; Nakanishi, F. *J. Phys. Chem. A* **2000**, *104*, 1827.
(46) Catalán, J.; Lopez, V.; Perez, P.; Martin-Villamil, R.; Rodriguez, J.-G. *Liebigs Ann.* **1995**, 241.
(47) Greenham, N. C.; Samuel, I. D. W.; Hayes, G. R.; Phillips, R. T.; Kessener, Y. A. R. R.; Moratti, S. C.; Holmes, A. B.; Friend, R. H. *Chem. Phys. Lett.* **1995**, *241*, 89.
(48) Rossi, R.; Ciofalo, M.; Carpita, A.; Ponterini, G. *J. Photochem. Photobiol. A Chem.* **1993**, *70*, 59.
(49) Ahlrichs, R. et al. TURBOMOLE version 5.6; University of Karlsruhe: Karlsruhe, Germany.
(50) Furche, F.; Ahlrichs, R. *J. Chem. Phys.* **2002**, *117*, 7433.
(51) Becke, A. D. *J. Chem. Phys.* **1993**, *98*, 5648.
(52) Schäfer, A.; Huber, C.; Ahlrichs, R. *J. Chem. Phys.* **1994**, *100*, 5829.
(53) Schäfer, A.; Huber, C.; Ahlrichs, R. *J. Chem. Phys.* **1992**, *97*, 2571.
(54) Turro, N. J. *Modern Molecular Photochemistry*; Benjamin/Cummings Publishing Company: Menlo Park, CA, 1978.
(55) Burin, A. L.; Ratner, M. A. *J. Chem. Phys.* **1998**, *109*, 6092.
(56) Lami, H.; Glasser, N. *J. Chem. Phys.* **1986**, *84*, 597.
(57) Englman, R.; Jortner, J. *Mol. Phys.* **1970**, *18*, 145.
(58) Bachilo, S. M.; Spangler, C. W.; Gillbro, T. *Chem. Phys. Lett.* **1998**, *283*, 235.